efficient filtration in liquid phase and the idea of critical point drying in order to prevent re-aggregation of the fibers by surface tension during drying. The latter step was inspired by the drying method for SEM samples. TB-sublimation technique used in this study is an alternative method used for SEM samples as well. Our trial-and-error added a few innovations such as gentle kneading of half-frozen TB suspension and a freeze-and-thaw process for a better dispersion (visible differences in fineness of suspension, data not shown), and vibration of the sieve for a faster and better yield of filtrate (approximately 7 fold increase in half the time). This Taquann method does not use high power sonication or other strong mechanical shearing, so that the length distribution of the single fibers did not change. The equipments and reagents used here are mostly available at regular biological or chemical laboratories. The new aerosol generating system by the direct injection of T-CNT had successfully generated highly dispersed aerosol of MWNT-7 and an exposure study confirmed the inhalation of MWNT-7 single fibers in mouse lung down to the peripheral alveolar spaces. In this condition, i.e. five consequtive days of 2 hr exposure, histologically, there were only mild neutrophilic infiltration. A long-term follow up study is underway.

It is highly plausible that the Taquann method can be applied to other types of particles as long as they are not soluble to TB (additional study in preparation). Well-dispersed samples generated by the Taquann method, together with the direct injection and the small scale inhalation chamber system, would facilitate the inhalation toxicity studies more relevant to human exposure not only at the big facilities but also at the small scaled laboratories.

Finally, this dispersion method may also be useful for industries where difficulty in dispersion of nanoparticles was a limiting process in developing new products. For a large scale manufacturing, carbon dioxide critical point drying may be suitable than TB sublimation.

## ACKNOWLEDGMENT

The authors thank Dr. Hiroyuki Tsuda for introducing the metal sieve for liquid phase filtration. This study is supported by the Health Sciences Research Grants H21-kagaku-ippan-008, H23-kagaku-ippan-005 and H24-kagaku-shitei-009 from the Ministry of Health, Labour and Welfare, Japan.

## REFERENCES

Ahn, K.H., Kim, S.M. and Yu, I.J. (2011): Multi-walled carbon nanotube (MWCNT) dispersion and aerosolization with hot water atomization without addition of any surfactant. Saf. Health Work., 2, 65-69.

Gasser, M., Wick, P., Clift, M.J., Blank, F., Diener, L., Yan, B., Gehr, P., Krug, H.F. and Rothen-Rutishauser, B. (2012): Pulmonary surfactant coating of multi-walled carbon nanotubes (MWCNTs) influences their oxidative and pro-inflammatory potential in vitro. Part Fibre Toxicol., 9, 17.

Han, J.H., Lee, E.J., Lee, J.H., So, K.P., Lee, Y.H., Bae, G.N., Lee, S.B., Ji, J.H., Cho, M.H. and Yu, I.J. (2008): Monitoring multi-walled carbon nanotube exposure in carbon nanotube research facility. Inhal. Toxicol., 20, 741-749.

Kasai, T., Gotoh, K., Nishizawa, T., Sasaki, T., Katagiri, T., Umeda, Y., Toya, T. and Fukushima, S. (2013): Development of a new multi-walled carbon nanotube (MWCNT) aerosol generation and exposure system and confirmation of suitability for conducting a single-exposure inhalation study of MWCNT in rats. Nanotoxicology, (in press).

Mercer, R.R., Hubbs, A.F., Scabilloni, J.F., Wang, L., Battelli, L.A., Friend, S., Castranova, V. and Porter, D.W. (2011): Pulmonary fibrotic response to aspiration of multi-walled carbon nanotubes. Part Fibre. Toxicol., 8, 21.

Mercer, R.R., Scabilloni, J., Wang, L., Kisin, E., Murray, A.R., Schwegler-Berry, D., Shvedova, A.A. and Castranova, V. (2008): Alteration of deposition pattern and pulmonary response as a result of improved dispersion of aspirated single-walled carbon nanotubes in a mouse model. Am. J. Physiol. Lung Cell. Mol. Physiol., 294, L87-97.

Mitchell, L.A., Gao, J., Wal, R.V., Gigliotti, A., Burchiel, S.W. and McDonald, J.D. (2007): Pulmonary and systemic immune response to inhaled multiwalled carbon nanotubes. Toxicol. Sci., 100, 203-214.

Morimoto, Y., Hirohashi, M., Ogami, A., Oyabu, T., Myojo, T., Todoroki, M., Yamamoto, M., Hashiba, M., Mizuguchi, Y., Lee, B.W., Kuroda, E., Shimada, M., Wang, W.N., Yamamoto, K., Fujita, K., Endoh, S., Uchida, K., Kobayashi, N., Mizuno, K., Inada, M., Tao, H., Nakazato, T., Nakanishi, J. and Tanaka, I. (2011): Pulmonary toxicity of well-dispersed multi-wall carbon nanotubes following inhalation and intratracheal instillation. Nanotoxicology, 6, 587-599.

Muller, J., Huaux, F., Moreau, N., Misson, P., Heilier, J.F., Delos, M., Arras, M., Fonseca, A., Nagy, J.B. and Lison, D. (2005): Respiratory toxicity of multi-wall carbon nanotubes. Toxicol. Appl. Pharmacol., 207, 221-231.

Oyabu, T., Myojo, T., Morimoto, Y., Ogami, A., Hirohashi, M., Yamamoto, M., Todoroki, M., Mizuguchi, Y., Hashiba, M., Lee, B.W., Shimada, M., Wang, W.N., Uchida, K., Endoh, S., Kobayashi, N., Yamamoto, K., Fujita, K., Mizuno, K., Inada, M., Nakazato, T., Nakanishi, J. and Tanaka, I. (2011): Biopersistence of inhaled MWCNT in rat lungs in a 4-week well-characterized exposure. Inhal. Toxicol., 23, 784-791.

Poland, C.A., Duffin, R., Kinloch, I., Maynard, A., Wallace, W.A., Seaton, A., Stone, V., Brown, S., Macnee, W. and Donaldson, K. (2008): Carbon nanotubes introduced into the abdominal cavity of mice show asbestos-like pathogenicity in a pilot study. Nat Nanotechnol., 3, 423-428.

Porter, D.W., Hubbs, A.F., Mercer, R.R., Wu, N., Wolfarth, M.G., Sriram, K., Leonard, S., Battelli, L., Schwegler-Berry, D.,

Friend, S., Andrew, M., Chen, B.T., Tsuruoka, S., Endo, M. and Castranova, V. (2009): Mouse pulmonary dose- and time course-responses induced by exposure to multi-walled carbon nanotubes. Toxicology, 269, 136-147.

Pott, F., Roller, M., Kamino, K. and Bellmann, B. (1994): Significance of durability of mineral fibers for their toxicity and carcinogenic potency in the abdominal cavity of rats in comparison with the low sensitivity of inhalation studies. Environ. Health Perspect., 102 Suppl. 5, 145-150.

Roller, M., Pott, F., Kamino, K., Althoff, G.H. and Bellmann, B. (1997): Dose-response relationship of fibrous dusts in intraperitoneal studies. Environ. Health Perspect., 105 Suppl. 5, 1253-1256.

Shvedova, A.A., Kisin, E., Murray, A.R., Johnson, V.J., Gorelik, O., Arepalli, S., Hubbs, A.F., Mercer, R.R., Keohavong, P., Sussman, N., Jin, J., Yin, J., Stone, S., Chen, B.T., Deye, G., Maynard, A., Castranova, V., Baron, P.A. and Kagan, V.E. (2008): Inhalation vs. aspiration of single-walled carbon nanotubes in C57BL/6 mice: inflammation, fibrosis, oxidative stress, and mutagenesis. Am. J. Physiol. Lung Cell. Mol. Physiol., 295, L552-565.

Takagi, A., Hirose, A., Futakuchi, M., Tsuda, H. and Kanno, J. (2012): Dose-dependent mesothelioma induction by intraperitoneal administration of multi-wall carbon nanotubes in p53 heterozygous mice. Cancer Sci., 103, 1440-1444.

Takagi, A., Hirose, A., Nishimura, T., Fukumori, N., Ogata, A., Ohashi, N., Kitajima, S. and Kanno, J. (2008): Induction of mesothelioma in p53+/- mouse by intraperitoneal application of multi-wall carbon nanotube. J. Toxicol. Sci., 33, 105-116.

Wang, X., Katwa, P., Podila, R., Chen, P., Ke, P.C., Rao, A.M., Walters, D.M., Wingard, C.J. and Brown, J.M. (2011): Multi-walled carbon nanotube instillation impairs pulmonary function in C57BL/6 mice. Part Fibre. Toxicol., 8, 24.

Wang, X., Xia, T., Duch, M.C., Ji, Z., Zhang, H., Li, R., Sun, B., Lin, S., Meng, H., Liao, Y.P., Wang, M., Song, T.B., Yang, Y., Hersam, M.C. and Nel, A.E. (2012): Pluronic F108 coating decreases the lung fibrosis potential of multiwall carbon nanotubes by reducing lysosomal injury. Nano Lett., 12, 3050-3061.

Warheit, D.B., Laurence, B.R., Reed, K.L., Roach, D.H., Reynolds, G.A. and Webb, T.R. (2004): Comparative pulmonary toxicity assessment of single-wall carbon nanotubes in rats. Toxicol. Sci., 77, 117-125.

Xu, J., Futakuchi, M., Shimizu, H., Alexander, D.B., Yanagihara, K., Fukamachi, K., Suzui, M., Kanno, J., Hirose, A., Ogata, A., Sakamoto, Y., Nakae, D., Omori, T. and Tsuda, H. (2012): Multi-walled carbon nanotubes translocate into the pleural cavity and induce visceral mesothelial proliferation in rats. Cancer Sci., 103, 2045-2050.

Cancer Science
The official journal of the Japanese Cancer Association JCA

# Dose-dependent mesothelioma induction by intraperitoneal administration of multi-wall carbon nanotubes in p53 heterozygous mice

Atsuya Takagi,[1] Akihiko Hirose,[2] Mitsuru Futakuchi,[3] Hiroyuki Tsuda[4] and Jun Kanno[1,5]

[1]Division of Cellular and Molecular Toxicology, [2]Division of Risk Assessment, Biological Safety Research Center, National Institute of Health Sciences, Tokyo; [3]Department of Molecular Toxicology, Nagoya City University Graduate School of Medical Sciences; [4]Nanomaterial Toxicology Project Laboratory, Nagoya City University, Nagoya, Japan

(Received February 21, 2012/Revised March 25, 2012/Accepted April 22, 2012/Accepted manuscript online April 27, 2012/Article first published online June 21, 2012)

**Among various types of multi-wall carbon nanotubes (MWCNT) are those containing fibrous particles longer than 5 μm with an aspect ratio of more than three (i.e. dimensions similar to mesotheliomagenic asbestos). A previous study showed that micrometer-sized MWCNT (μm-MWCNT) administered intraperitoneally at a dose of 3000 μg/mouse corresponding to $1 \times 10^9$ fibers per mouse induced mesotheliomas in p53 heterozygous mice. Here, we report a dose-response study; three groups of p53 heterozygous mice ($n = 20$) were given a single intraperitoneal injection of 300 μg/mouse of μm-MWCNT (corresponding to $1 \times 10^8$ fibers), 30 μg/mouse ($1 \times 10^7$) or 3 μg/mouse ($1 \times 10^6$), respectively, and observed for up to 1 year. The cumulative incidence of mesotheliomas was 19/20, 17/20 and 5/20, respectively. The severity of peritoneal adhesion and granuloma formation were dose-dependent and minimal in the lowest dose group. However, the time of tumor onset was apparently independent of the dose. All mice in the lowest dose group that survived until the terminal kill had microscopic atypical mesothelial hyperplasia considered as a precursor lesion of mesothelioma. Right beneath was a mononuclear cell accumulation consisting of CD45- or CD3-positive lymphocytes and CD45/CD3-negative F4/80 faintly positive macrophages; some of the macrophages contained singular MWCNT in their cytoplasm. The lesions were devoid of epithelioid cell granuloma and fibrosis. These findings were in favor of the widely proposed mode of action of fiber carcinogenesis, that is, frustrated phagocytosis where the mesotheliomagenic microenvironment on the peritoneal surface is neither qualitatively altered by the density of the fibers per area nor by the formation of granulomas against agglomerates. (*Cancer Sci* 2012; 103: 1440–1444)**

Unique properties such as persistency and electric conductivity promise a high potential for technology applications of carbon nanotubes (e.g. in lithium ion batteries). Immediately after the invention of the carbon nanotube, its persistency and fibrous shape have posed a challenge for toxicology known as "fiber carcinogenesis".[1] A recent study showed that a particular type of multi-wall carbon nanotube (Mitsui MWCNT-7, designated in general here as micrometer-sized MWCNT or μm-MWCNT) contains a considerable percentage of particles similar to asbestos in length and diameter.[2] To investigate its mesotheliomagenic potential, we used an intraperitoneal injection (i.p.) method that was extensively used in the 1970s and 1980s for the elucidation of key dimensions of the fiber (e.g. length and diameter) and for toxicity assessment of various man-made fibers.[3–6] Although the route of exposure is not realistic for humans, the i.p. injection method has been considered appropriate to assess the mesotheliomagenic potential of fibers,[7] and the least potent fibers were found to induce a positive result at a dose of $10^9$ fibers i.p. in rats.[6–8]

Our first study identified the mesotheliomagenic potency of Mitsui MWCNT-7 at a single maximum dose (i.e. $10^9$ fibers) in the peritoneal cavity of p53 heterozygous (p53+/−) mice[2] (data shown as a reference in Fig. 1). Marsella *et al.*[9] has shown that development of mesothelioma by crocidolite asbestos was accelerated in this mutant mouse. We have bred this mouse and tested it as an alternative model to replace the wild-type mouse carcinogenicity test of the National Toxicology Program of the National Institute of Environmental Health Sciences/NIH of the United States.[10] As a result, spontaneous neoplastic lesions of this model have been well characterized.[11]

Here, we applied the same fiber to p53+/− mice at doses of 1/10, 1/100, and 1/1000 of the dose used in the previous study (i.e. 300, 30 and 3 μg/mouse), which corresponds to approximately $1 \times 10^8$, $1 \times 10^7$, and $1 \times 10^6$ fibers per mouse, respectively, and monitored the mice for 1 year.

## Materials and Methods

**Experimental animals.** The p53+/− mice were generously supplied by Dr S. Aizawa,[12] and back crossed with normal wild-type C57BL/6 females (SLC, Shizuoka, Japan) for more than 20 generations at the National Institute of Health Sciences (NIHS), Tokyo. Eighty male p53+/− mice aged 9–11 weeks were divided into four groups of 20 mice, and housed individually under specific pathogen-free conditions with a 12-h light-dark cycle at a NIHS animal facility. They were given tap water and autoclaved CRF-1 pellets (Oriental Yeast Co. Ltd., Tokyo, Japan) *ad libitum*. Experiments were humanely conducted under the regulation and permission of the Animal Care and Use Committee of the NIHS.

**Histology.** Liver, kidney, spleen, lung, digestive tract and macroscopic tumors (*en bloc* in the case of severe peritoneal adhesion) were fixed in 10% neutral buffered formalin. After conventional processing, paraffin-embedded sections were stained with hematoxylin–eosin (HE) and examined histopathologically under a light microscope. A pair of polarizing filters was set to a light microscope to detect birefringent particles.

For the selected atypical mesothelial hyperplasia lesions, serial sections were stained for CD45R(B220), CD3 and F4/80 using anti-mouse CD45R (eBioscience, San Diego, CA, USA), anti-rat CD3 (AbD Serotec, Kidlington, UK), anti-mouse F4/80 antibodies (eBioscience), which were diluted at 1:100, 1:50 and 1:50, respectively. The slides were incubated at 4°C overnight

[5]To whom correspondence should be addressed.
E-mail: kanno@nihs.go.jp


doi: 10.1111/j.1349-7006.2012.02318.x

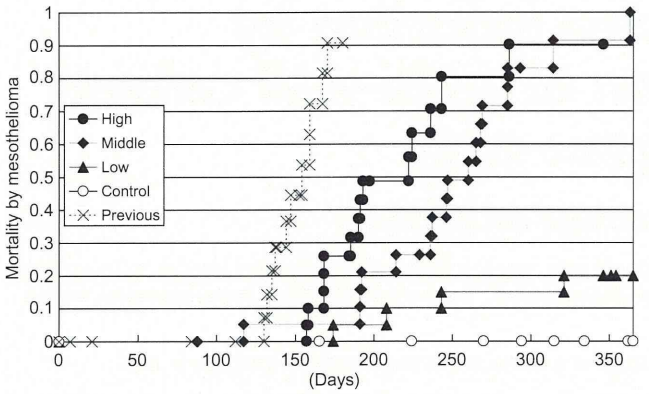


**Fig. 1.** Dose-dependent induction of mesotheliomas by micrometer-sized multi-wall carbon nanotubes (μm-MWCNT). Mice with lethal mesotheliomas are plotted using the Kaplan–Meier method. High: 300 μg/mouse, corresponding to $1 \times 10^8$ fibers/mouse; middle: 30 μg/mouse, corresponding to $1 \times 10^7$ fibers/mouse; low: 3 μg/mouse, corresponding to $1 \times 10^6$ fibers/mouse); previous: data from a previous study (i.e. 3 mg/mouse, corresponding to $1 \times 10^9$ fibers/mouse). No mesothelioma was observed in the vehicle control group.

and then incubated for 1 h with biotinylated species-specific secondary antibodies diluted 1:500 (Vector Laboratories, Burlingame, CA, USA) and visualized using avidin-conjugated alkaline phosphatase complex (ABC kit; Vector Laboratories).

**Test material.** Multi-wall carbon nanotube (MITSUI MWCNT-7, Lot No. 060125-01k), the same lot used in our previous study[2] was used. As reported in our previous paper, one gram of MWCNT corresponded to $3.55 \times 10^{11}$ particles. The length ranged from 1 to 20 μm with a median of 2 μm. More than 25% of the particles were longer than 5 μm; their width ranged from 70 to 170 nm with a median of 90 nm. The approximate average content of iron was 3500 ppm (0.35%) and that of sulfur was 470 ppm. The concentration of chlorine in the fibers was 20 ppm and that of fluorine and bromine was below the limits of detection (5 and 40 ppm, respectively).[2]

Multi-wall carbon nanotubes was suspended at a concentration of 3 mg/mL to 0.5% methyl cellulose (Shin-Etsu Chemical Co. Ltd, Tokyo, Japan) solution and autoclaved (121°C, 15 min). After addition of Tween 80 (Tokyo Chemical Industry Co. Ltd, Tokyo, Japan; final 1.0% concentration), the solution was subjected to sonication at 150 watt for 5 min using an ultrasonic homogenizer (VP30s; TAITEC Co., Saitama, Japan).

**Treatment.** Eighty male p53+/− mice aged 9–11 weeks were randomly divided into four groups of 20. The high-dose group mice were given a single i.p. injection of 300 μg/mouse of MWCNT particles (corresponding to $1 \times 10^8$ fibers) in 1 mL suspension. The middle-dose group mice received 30 μg/mouse ($1 \times 10^7$) and the low-dose group mice received 3 μg/mouse ($1 \times 10^6$), respectively. The control group mice received vehicle solution (1 mL). Treated mice were monitored for 1 year. To minimize stress to the animals and re-aggregation of suspension, the injection was promptly performed without anesthesia.

## Results

Peritoneal mesotheliomas were induced in a dose-dependent manner shown by an increase in the cumulative incidence of the tumors (Fig. 1). In the high-dose group, 14/20 mice had single or multiple lethal mesotheliomas up to 2 × 2 cm in size located within the peritoneal cavity, invading adjacent organs and structures with or without peritoneal dissemination. The remaining mice died of ileus due to severe peritoneal adhesion and fibrosis, and among them five had small incidental (non-lethal) mesotheliomas. The total incidence of mesothelioma was 19/20 (95%) among the animals. These lesions were qualitatively identical to our previous study.[2] In the middle-dose group, 17/20 (85%) mice had lethal mesothelioma. Three mice without lethal mesothelioma died or became moribund due to other reasons including leukemia. In the low-dose group, 4/20 mice had lethal mesothelioma (Fig. 2) and 1/20 had a non-lethal mesothelioma (found at the terminal kill on day 365), which makes the overall incidence of mesothelioma 5/20 (25%). The other 15 mice that survived until the terminal kill showed focal mesothelial atypical hyperplasia.[13] These lesions, up to 0.5 mm in diameter, consisted of a single layer of mesothelium characterized by cuboidal or hobnail appearance with slight to moderate nuclear atypia. Right beneath the

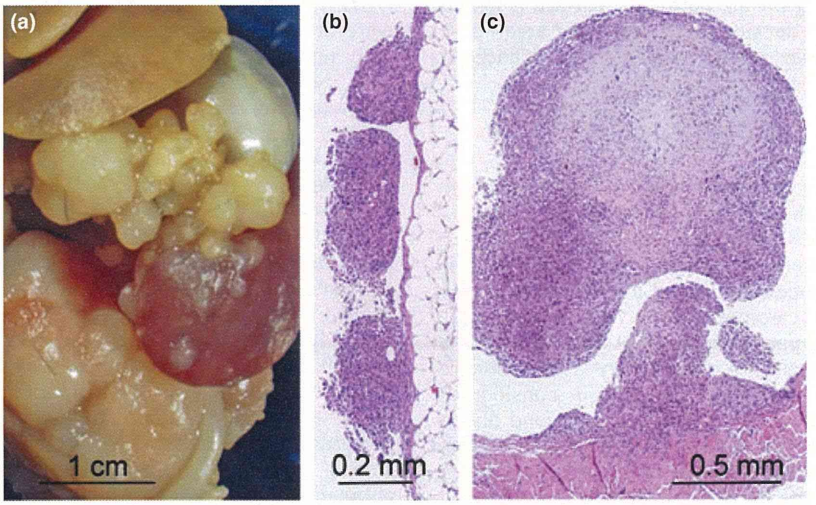


**Fig. 2.** Morphology of the induced mesotheliomas in the low-dose group. (a) Macroscopic view of the abdominal cavity of a mouse in the low-dose group. Multiple nodules are seen on the surface of the peritoneal serosa. This mouse died on day 243 with multiple nodules up to size 1 × 1 × 1 cm. (b) Low-power light microscopy view of the multiple nodules on the peritoneal surface of the mesentery. Granulomas and fibrous scars are minimal in the low-dose group. (c) Histology of a small nodule compatible with a diagnosis of moderately to poorly differentiated epithelioid mesothelioma. Larger nodules tended to be composed of undifferentiated sarcomatous components.[2]

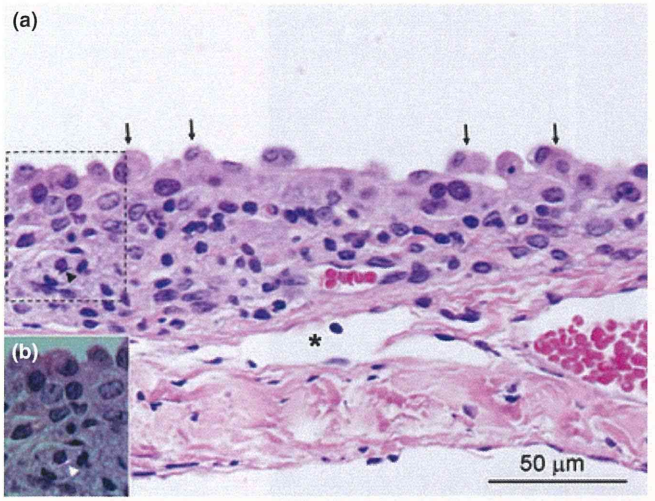


**Fig. 3.** Atypical mesothelial hyperplasia. (a) Atypical mesothelial hyperplasia of the tendinous portion of the diaphragm of a mouse in the low-dose group (sampled at terminal kill, that is, 365 days after i. p. inoculation of the multi-wall carbon nanotubes [MWCNT]). Arrows: hobnail appearance of the atypical hyperplastic mesothelial cells; asterisk: lymphatic drainage of the peritoneal cavity. (b) Polarized image of the dotted area in (a). Arrowhead: a MWCNT fiber in a macrophage-like cell (birefringent).

atypical mesothelium was a lentiform accumulation of mononuclear inflammatory cells up to 0.1 mm in thickness (Fig. 3). The accumulation is a combination of ill-demarcated zones of CD45-positive lymphocytes, CD3-positive lymphocytes and CD45/CD3-negative F4/80-negative or CD45/CD3-negative F4/80 weakly positive macrophage-like cells (Fig. 4). Single MWCNT fiber was often found in the cytoplasm of the macrophage-like cells. These lesions were devoid of epithelioid cell granuloma and fibrous scars.

Peritoneal fibrosis, peritoneal adhesion and formation of foreign body granulomas towards agglomerated MWCNT were dose dependent and minimal in the low-dose group. In the control group, mesotheliomas were not found (0%). There were eight mice with lethal or incidental thymic lymphoma, leukemia or reticulum cell sarcoma, osteosarcoma of the cranial bone, and 12/20 were tumor free. These tumors are known to develop spontaneously in p53+/− mice with increasing age[10] and none of these tumors were treatment dependent.

Histology of the mesotheliomas ranged from a differentiated epithelioid type to an undifferentiated sarcomatous type. Osteoid and rhabdoid differentiations, both known in human cases,[14–16] were found in nine mice (two in the low dose, three in the middle dose, and four in the high dose group, respectively) among a total of 41 mesothelioma cases in the present study.

An additional finding was the dissemination of singular fibers to systemic organs such as the liver, mesenteric lymph nodes, pulmohilar lymph nodes, choroid plexus of the brain, glomeruli of the kidney and lung alveoli (Fig. 5). Because the brain, including the choroid plexus, lacks afferent lymphatics,[17,18] it is probable that the fibers were distributed systemically via the blood stream.

## Discussion

The present study showed a dose-dependent induction of mesothelioma by the μm-MWCNT from 1/1000 of the dose of our previous study (i.e. 3 μg/mouse corresponding to $1 \times 10^6$ fibers).

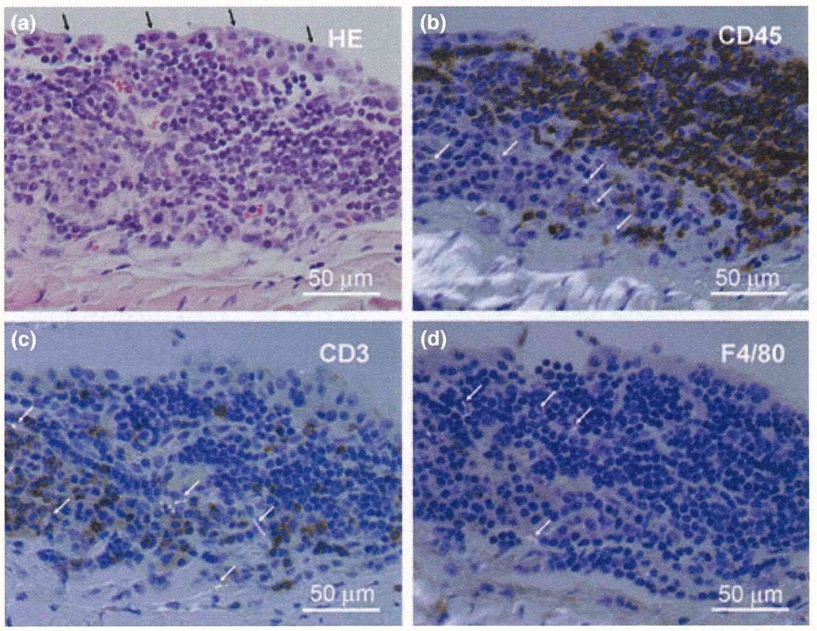


**Fig. 4.** Immunohistochemistry of lentiform mononuclear cell accumulation underlying the atypical mesothelial hyperplasia. (a) Serial section of an atypical mesothelial hyperplasia of the tendinous portion of the diaphragm of a mouse in the low-dose group (sampled at terminal kill). (a) Hematoxylin–eosin staining. Black arrows: hobnail appearance of the hyperplastic mesothelial cells. (b–d) Polarized image of the serial sections immunohistochemically stained for CD45, CD3 and F4/80. Multi-wall carbon nanotubes (birefringent; white arrows) are seen in the macrophage-like CD45/CD3-negative, F4/80-faintly positive cell cytoplasm. It is noted that epithelioid cell granuloma and fibrous scars are absent in this type of lesion.



doi: 10.1111/j.1349-7006.2012.02318.x

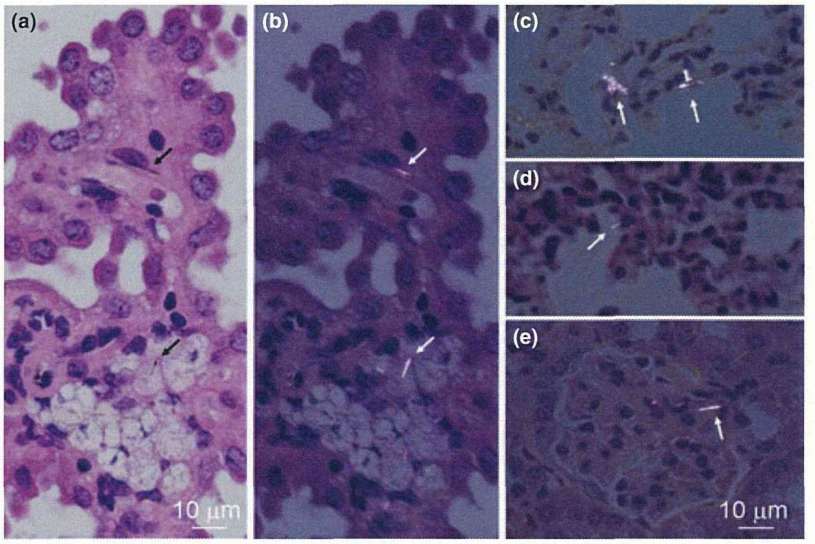


**Fig. 5.** Systemic distribution of singular fibers. Single micrometer-sized multi-wall carbon nanotube fibers are found in the choroid plexus in (a) normal lighting and (b) polarized light (in a mouse from the high-dose group sampled on day 168), (c) lung as an agglomerate within macrophages (polarized light) or (d) as singular fibers (polarized light) and (e) a renal glomerulus (polarized light) (in a mouse from the high-dose group sampled on day 197). Fibers were also found in hepatic sinusoids and mesenteric lymph nodes (not shown).

It is noted that the mesotheliomas of the low-dose group were not accompanied by foreign body granulomas or fibrous scars. The mesothelial atypical hyperplasia found 1 year after the i.p. injection in the low-dose group mice were also devoid of foreign body granulomas and fibrous scars. Instead, these lesions were backed up by an accumulation of mononuclear inflammatory cells. The macrophage-like cells in the accumulation, negative to weakly positive for F8/40, were often positive for singular MWCNT in their cytoplasm. As the mesothelial atypical hyperplasia is considered as precancerous lesions, the essential background of mesotheliomagenesis might be the inflammatory lesions without granulomas and fibrous scars formed against MWCNT agglomerates. The mesothelial atypical hyperplasia can be regarded as a lesion driven by the frustrated phagocytosis against MWCNT.

In general, carcinogenesis is considered a multistage process. In the case of chemical carcinogens with clear genotoxic properties, tumor onset occurs significantly earlier at higher doses.[19,20] Presumably, an increasing number of hits to a target cell leads to faster progression of the carcinogenic stages. Here, in contrast, the onset time of the mesotheliomas was apparently dose independent. Onset estimates calculated as x-intercepts of logarithmic approximation[21,22] were 126, 146, 148 and 138 days for the previous study data[2] and the three doses of the present study, respectively (Fig. S1). Mechanistically, a direct effect to a mesothelial cell, such as mutagenic or clastogenic effect, would favor a dose-dependent acceleration of the onset. If the granulomas are an important promoting factor of mesotheliomagenesis,[23] the highest dose group should have had the earliest onset because the granuloma formation can take place within 7 days subsequent to the i.p. injection.[24] In contrast, the humoral stimuli released from the nearby macrophages in the condition of frustrated phagocytosis[25] would match with this finding. As shown in Figures 3 and 4, the reactive mesothelial cells are accompanied by mononuclear inflammatory cells with MWCNT fibers, but not by epithelioid cell granulomas or fibrous scars. One could speculate that each loci of frustrated phagocytosis could continuously stimulate the nearby mesothelial cells, that is, first to induce reactive hyperplasia and then as the next step proceed towards mesothelioma. If the dose is the determinant of the number of such loci within a defined surface area of peritoneal mesothelial membrane, then it is natural to predict that the earliest day of tumor onset is dose independent, whereas the probability of tumor onset closer to the earliest day will increase in a dose-dependent manner.

An additional finding was the distribution of singular fibers to systemic organs such as the liver, mesenteric lymph nodes, pulmohilar lymph nodes, choroid plexus of the brain, glomeruli of the kidney and lung alveoli (Fig. 5). Because the brain, including the choroid plexus, lacks afferent lymphatics,[17,18] it is probable that the fibers were distributed systemically via the blood stream. Its importance to human health could be closely linked to the systemic distribution of asbestos reported in humans,[26,27] that is, a possibility of increasing systemic diseases such as cancer in various organs[28] and autoimmune diseases.[29] *In vivo* studies on the shorter fractions of MWCNT for its systemic toxicity would be essential.

It is likely that the peritoneal cavity served as a filter to segregate large agglomerates from the i.p. injected MWCNT suspension by the formation of foreign body granulomas and fibrous scars, leaving singular long MWCNT fibers for mesotheliomagenesis (frustrated phagocytosis) and short singular fibers for systemic distribution. The short fibers might have passed through the stomata (pores) of the mesothelium[23] or been transported by macrophages into lymphatics and to the vascular systems. As a whole, the i.p. injection model appears to be a robust system for the hazard identification of fiber carcinogenesis of asbestos-like fibrous particulate matter and of systemic toxicity of fibrous and non-fibrous particulate matter including nanoparticles that can enter the blood stream.

In conclusion, μm-MWCNT was mesotheliomagenic in the p53+/− mouse peritoneal cavity model in a dose-dependent manner from as low as 3 μg per mouse or approximately $10^6$ fibers per mouse. Although the molecular mechanisms of fiber mesotheliomagenesis are unknown, the minute lesions seen in the lowest dose group and the dose-response characteristics might be consistent with the concept of frustrated phagocytosis and also with the observation in human asbestos epidemiology

that there would be no practical threshold for fiber mesotheliomagenesis.


## Acknowledgments

The authors thank Mr Masaki Tsuji for technical support, and Dr Robert R. Maronpot and Dr Kai Savolainen for critical reading of the manuscript. The present study was supported by Health Sciences Research Grants H18-kagaku-ippan-007 and H21-kagaku-ippan-008 from the Ministry of Health, Labour and Welfare, Japan.


## Disclosure Statement

The authors have no conflict of interest.

## References


1 Service RF. CHEMISTRY: nanotubes: the next asbestos? *Science* 1998; **281**: 941.
2 Takagi A, Hirose A, Nishimura T *et al.* Induction of mesothelioma in p53+/− mouse by intraperitoneal application of multi-wall carbon nanotube. *J Toxicol Sci* 2008; **33**: 105–16.
3 Stanton MF, Layard M, Tegeris A *et al.* Relation of particle dimension to carcinogenicity in amphibole asbestoses and other fibrous minerals. *J Natl Cancer Inst* 1981; **67**: 965–75.
4 Pott F, Roller M, Kamino K, Bellmann B. Significance of durability of mineral fibers for their toxicity and carcinogenic potency in the abdominal cavity of rats in comparison with the low sensitivity of inhalation studies. *Environ Health Perspect* 1994; **102**(Suppl 5): 145–50.
5 Adachi S, Yoshida S, Kawamura K *et al.* Inductions of oxidative DNA damage and mesothelioma by crocidolite, with special reference to the presence of iron inside and outside of asbestos fiber. *Carcinogenesis* 1994; **15**: 753–8.
6 Roller M, Pott F, Kamino K, Althoff GH, Bellmann B. Dose-response relationship of fibrous dusts in intraperitoneal studies. *Environ Health Perspect* 1997; **105**(Suppl 5): 1253–6.
7 World Health Organization. *WHO Workshop on Mechanisms of Fibre Carcinogenesis and Assessment of Chrysotile Asbestos Substitutes*, 8–12 November 2005. Lyon, France: Summary Consensus Report World Health Organization, 2006.
8 European Chemicals Bureau. Carcinogenicity of synthetic mineral fibres after intraperitoneal injection in rats (ECB/TM/18(97) rev. 1). In: Bernstein DM, Riego Sintes JM, eds. *Methods for the Determination of the Hazardous Properties for Human Health of Man Made Mineral Fibres (MMMF) (EUR 18748 EN [1999])*. Ispra, Italy: Institute for Health and Consumer Protection, Unit: Toxicology and Chemical Substances, 1999; 41–52. [Cited 26 May 2012.] Available from URL: http://tsar.jrc.ec.europa.eu/documents/Testing-Methods/mmmfweb.pdf.
9 Marsella JM, Liu BL, Vaslet CA, Kane AB. Susceptibility of p53-deficient mice to induction of mesothelioma by crocidolite asbestos fibers. *Environ Health Perspect* 1997; **105**(Suppl 5): 1069–72.
10 Mahler JF, Flagler ND, Malarkey DE, Mann PC, Haseman JK, Eastin W. Spontaneous and chemically induced proliferative lesions in Tg.AC transgenic and p53-heterozygous mice. *Toxicol Pathol* 1998; **26**: 501–11.
11 Eastin WC, Haseman JK, Mahler JF, Bucher JR. The National Toxicology Program evaluation of genetically altered mice as predictive models for identifying carcinogens. *Toxicol Pathol* 1998; **26**: 461–73.
12 Tsukada T, Tomooka Y, Takai S *et al.* Enhanced proliferative potential in culture of cells from p53-deficient mice. *Oncogene* 1993; **8**: 3313–22.
13 Chung A, Cagle PT, Roggli VL, eds. *Tumors of the Serosal Membranes*. Washington, DC: American Registry of Pathology, 2006.
14 Chalabreysse L, Guillaud C, Tabib A, Loire R, Thivolet-Bejui F. Malignant mesothelioma with osteoblastic heterologous elements. *Ann Pathol* 2001; **21**: 428–30.
15 Matsukuma S, Aida S, Hata Y, Sugiura Y, Tamai S. Localized malignant peritoneal mesothelioma containing rhabdoid cells. *Pathol Int* 1996; **46**: 389–91.
16 Ordonez NG. Mesothelioma with rhabdoid features: an ultrastructural and immunohistochemical study of 10 cases. *Mod Pathol* 2006; **19**: 373–83.
17 Courtice FC, Simmonds WJ. The removal of protein from the subarachnoid space. *Aust J Exp Biol Med Sci* 1951; **29**: 255–63.
18 Weller RO, Djuanda E, Yow HY, Carare RO. Lymphatic drainage of the brain and the pathophysiology of neurological disease. *Acta Neuropathol* 2009; **117**: 1–14.
19 National Toxicology Program. NTP technical report on the toxicology and carcinogenesis studies of dimethyl vinyl chloride (L-chloro-2-methylpropene) (Cas No. 513-37-1) in F344/N rats and B6C3F1 mice (Gavage Studies) (NTP TR 316). National Toxicology Program, Research Triangle Park, North Carolina, 1986. [Cited 26 May 2012.] Available from URL: http://ntp.niehs.nih.gov/ntp/htdocs/lt_rpts/tr316.pdf.
20 National Toxicology Program. NTP technical report on the toxicology and carcinogenesis studies of glycidol (Cas No. 556-52-5) in F344/N rats and B6C3F1 mice (Gavage Studies) (NTP TR 374). National Toxicology Program, Research Triangle Park, North Carolina, 1990. [Cited 26 May 2012.] Available from URL: http://ntp.niehs.nih.gov/ntp/htdocs/LT_rpts/tr374.pdf.
21 Boffetta P, Burdorf A, Goldberg M, Merler E, Siemiatycki J. Towards the coordination of European research on the carcinogenic effects of asbestos. *Scand J Work Environ Health* 1998; **24**: 312–7.
22 Yano E, Wang ZM, Wang XR, Wang MZ, Lan YJ. Cancer mortality among workers exposed to amphibole-free chrysotile asbestos. *Am J Epidemiol* 2001; **154**: 538–43.
23 Donaldson K, Murphy FA, Duffin R, Poland CA. Asbestos, carbon nanotubes and the pleural mesothelium: a review of the hypothesis regarding the role of long fibre retention in the parietal pleura, inflammation and mesothelioma. *Part Fibre Toxicol* 2010; **7**: 5.
24 Poland CA, Duffin R, Kinloch I *et al.* Carbon nanotubes introduced into the abdominal cavity of mice show asbestos-like pathogenicity in a pilot study. *Nat Nanotechnol* 2008; **3**: 423–8.
25 Nagai H, Toyokuni S. Biopersistent fiber-induced inflammation and carcinogenesis: lessons learned from asbestos toward safety of fibrous nanomaterials. *Arch Biochem Biophys* 2010; **502**: 1–7.
26 Tossavainen A, Karjalainen A, Karhunen PJ. Retention of asbestos fibers in the human body. *Environ Health Perspect* 1994; **102**(Suppl 5): 253–5.
27 Miserocchi G, Sancini G, Mantegazza F, Chiappino G. Translocation pathways for inhaled asbestos fibers. *Environ Health* 2008; **7**: 4.
28 Goldsmith JR. Asbestos as a systemic carcinogen: the evidence from eleven cohorts. *Am J Ind Med* 1982; **3**: 341–8.
29 Noonan CW, Pfau JC, Larson TC, Spence MR. Nested case-control study of autoimmune disease in an asbestos-exposed population. *Environ Health Perspect* 2006; **114**: 1243–7.


## Supporting Information

Additional Supporting Information may be found in the online version of this article:

**Fig. S1.** Estimation of the time of tumor onset.

Please note: Wiley-Blackwell are not responsible for the content or functionality of any supporting materials supplied by the authors. Any queries (other than missing material) should be directed to the corresponding author for the article.



doi: 10.1111/j.1349-7006.2012.02318.x

—Review—

# ナノマテリアルの慢性影響研究の重要性

広瀬明彦,*,[a] 高木篤也,[a] 西村哲治,[a] 津田洋幸,[b] 坂本義光,[c]
小縣昭夫,[c] 中江　大,[c] 樋野興夫,[d] 菅野　純[a]

# Importance of Researches on Chronic Effects by Manufactured Nanomaterials

Akihiko HIROSE,*,[a] Atsuya TAKAGI,[a] Tetsuji NISHIMURA,[a]
Hiroyuki TSUDA,[b] Yoshimitsu SAKAMOTO,[c] Akio OGATA,[c]
Dai NAKAE,[c] Okio HINO,[d] and Jun KANNO[a]

[a]Division of Risk Assessment, National Institute of Health Sciences, Kamiyoga 1-18-1, Setagaya-ku, Tokyo 158-8501, Japan, [b]Nagoya City of University, 1 Kawasumi Mizuho-cho, Mizuho-ku, Nagoya 467-8601, Japan, [c]Tokyo Metropolitan Institute of Public Health, 3-24-1 Hyakunin-cho, Shinjyuku-ku, Tokyo 169-0073, Japan, and [d]Juntendo University School of Medicine, 2-1-1 Hongo, Bunkyo-ku, Tokyo 113-8421, Japan

(Received September 3, 2010)

Manufactured nanomaterials are the most important substances for the nanotechnology. The nanomaterials possess different physico-chemical properties from bulk materials. The new properties may lead to biologically beneficial effects and/or adverse effects. However, there are no standardized evaluation methods at present. Some domestic research projects and international OECD programs are ongoing, in order to share the health impact information of nanomaterails or to standardize the evaluation methods. From 2005, our institutes have been conducting the research on the establishment of health risk assessment methodology of manufactured nanomaterials. In the course of the research project, we revealed that the nanomaterials were competent to cause chronic effects, by analyzing the intraperitoneal administration studies and carcinogenic promotion studies. These studies suggested that even aggregated nanomaterials were crumbled into nano-sized particles inside the body during the long-term, and the particles were transferred to other organs. Also investigations of the toxicokinetic properties of nanomaterials after exposure are important to predict the chronically targeted tissues. The long lasting particles/fibers in the particular tissues may cause chronic adverse effects. Therefore, focusing on the toxicological characterization of chronic effects was considered to be most appropriate approach for establishing the risk assessment methods of nanomaterials.

Key words——chronic toxicity; multi-wall carbon nanotube (MWCNT); fullerene

## 1. はじめに

近年，ナノテクノロジーの中心的な役割を担う物質としての産業用ナノマテリアルは，急速にその種類や生産量が増加しつつあるところであるが，新たに期待されているナノマテリアルの物理化学特性については，有効的な生理活性等に使用され得る特性を持つ反面，ヒト健康影響に対する懸念についても検証されるべきであると考えられている．つまり，ナノマテリアルを用いた技術や製品を社会的に受容するためには，安全性の検証を行うことが不可欠であると思われる．しかし，従来の一般的な化学物質とは異なる物理化学的特性は，その毒性評価においても従来とは異なる考え方を取り入れることも必要とされている．それゆえ，ナノマテリアルの特性を考慮した有害性評価手法の開発が急務となっている．また，国際的な枠組みにおいても，ナノマテリアルの安全性確認は，重要な問題として認識されており，OECDやISO等を中心として評価手法の国際的標準化に向けた取り組みが進行しているところでもある．本稿では，ナノマテリアルの安全性評価

[a]国立医薬品食品衛生研究所（〒158-8501 東京都世田谷区上用賀 1-18-1），[b]名古屋市立大学（〒467-8601 名古屋市瑞穂区瑞穂町字川澄 1），[c]東京都健康安全研究センター（〒169-0073 東京都新宿区百人町 3-24-1），[d]順天堂大学医学部（〒113-8421 東京都文京区本郷 2-1-1）
*e-mail: hirose@nihs.go.jp

本総説は，日本薬学会第130年会シンポジウムS18で発表したものを中心に記述したものである．

の確立に向けたこれらの取り組みに貢献してきたわれわれの研究成果の一部と，それらの研究結果から帰納的に導き出された慢性影響評価研究の重要性について論ずる．

## 2. ナノマテリアルのリスク評価法の確立における課題

一般的に，化学物質の健康影響評価（リスクアセスメント）の基本的なフレームは，有害性評価と曝露評価，及び各々の評価内容を比較・統合化する過程のリスク判定のステップから成り立っている．この基本的なフレーム自体は，ナノマテリアルの健康影響評価に適用できるものであると考えられる．[1-5] しかし，ナノマテリアルに特徴的な新たな物理化学的性質，特にサイズが生体内高分子と近いことや，高い表面活性のために凝集し易い性質を考慮すると，よりサイズの大きい通常のバルク化合物や完全に溶解した単一分子化合物とは，生体内挙動が異なることが予想され，同じ化学組成の化合物であってもその毒性発現部位や発現様式は異なることが予想される．つまり，体内動態［吸収 absorption，分布 distribution，代謝 metabolism，排泄 excretion (ADME)］情報は，一般の化学物質より重要な意味を持つと考えられる．

そこで，生体内での挙動を把握するためには，生体試料中で検出，同定・定量できる方法を確立しなくてはならない．一般にナノマテリアルの開発段階において，その性質を把握するための物理化学的測定法も同時に開発されているはずであるが，それらの手法は生体試料中に存在するナノマテリアルにそのまま適用できないことも多い．さらに，機器分析法による生体試料中での検出や定量が可能になったとしても，生体内で実際にナノの状態で存在しているのか，あるいは再凝集などはしていないかなど，標的組織における最終的な生体内反応に影響を及ぼすと考えられる実際のナノマテリアルの存在状態を把握するためには，最終的には，組織標本の電子顕微鏡などによる確認が必要となる．

一方，体内動態に影響を与える因子として，投与法を検討する必要もある．単独では凝集し易いナノマテリアルをそのまま曝露するということは，物理的に巨大となった粒子は体への吸収性が低く，ナノマテリアル自体の体内動態や懸念される有害性を検出することが困難になると考えられるためである．そのために曝露実験時におけるナノマテリアルの分散手法の開発が必要となる．職業曝露などの比較的大量のナノマテリアル曝露の安全性を評価するという観点からは，凝集したままの曝露にも意義があるかもしれないが，製品中への混入や環境中への排出を経由した，分散された曝露も想定されることは考慮すべきであると考えられる．

Figure 1は，凝集したナノマテリアルが，生体に取り込まれた場合に想定される体内動態を模式図化したものである．ナノマテリアルの使用用途にも依存するが，製品中のナノマテリアルはポリマー等の他の高分子化合物等と混合された状態，あるいはナノマテリアルだけが単独で製品から解離していく状態を考慮しても，この凝集性のために，大きな粒子として曝露する可能性が高いものと想定される．急性的には，このサイズの大きくなった物質は生体に取り込まれることはほとんどなく，局所的な刺激を起こすような変化を除いては，生体内で有害性が惹起される可能性は低いものと考えられる．しかし，仮に凝集したナノマテリアルが長期間に渡って，吸収部位である肺胞や消化管，損傷皮膚などの局所に滞留したり，慢性的に曝露したりするケースを想定すると，時間経過とともに小さくなった凝集体の粒子を除去するために，マクロファージなどの食細胞による取り込みや，表面活性の高いナノマテリアル分子と生体成分との結合作用による侵食作用により，生体に少しずつ取り込まれることが想定される．もしも生体内に取り込まれたナノマテリアルと生体内成分との結合性が高い場合には，容易に生体外に排出されることはなく，特定の組織等へ蓄積し易くなり，慢性影響の可能性を検討する必要が出てくると想定できる．

## 3. 国立医薬品食品衛生研究所における取り組みの成果の概要

以上のナノマテリアル固有の検討課題を考慮して，われわれは2005年より厚生労働科学研究の化学物質リスク研究事業の枠組みの中で，ナノマテリアルの健康影響評価手法の開発に係わる研究を推し進めてきたところである．われわれは，これらの検討課題を解決するために，Fig. 2に示すように4つの項目を中心に研究を行ってきた．これらの項目の中で，in vivo 研究については，比較的研究初期の段階から中心的に取り組んできた．その中で，繊維

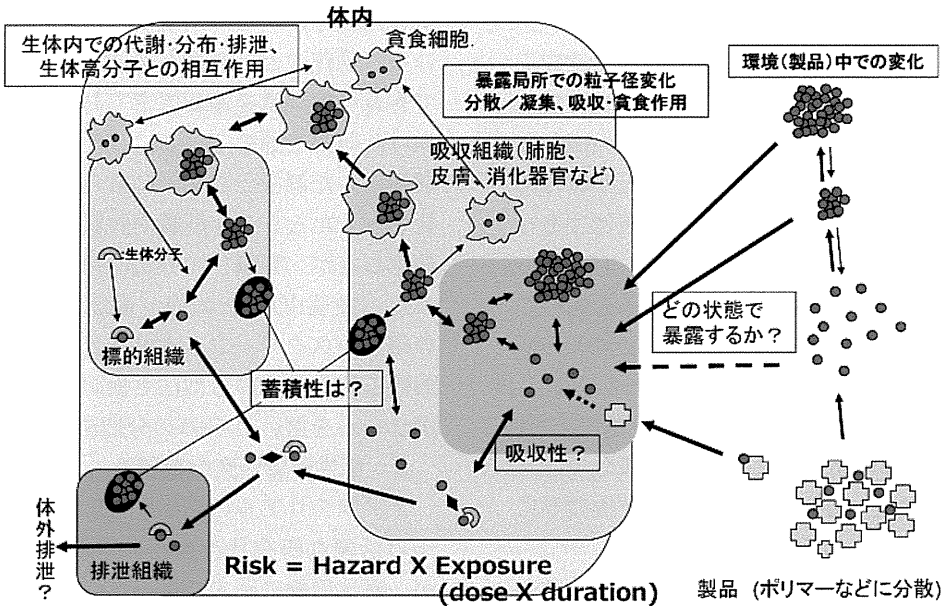


Fig. 1. The Estimated ADME Schema of Nanomaterials

***in vivo*試験法研究**

MWCNTのP53ヘテロ欠失マウスへのi.p.投与による中皮腫誘発性を確認

バイオマーカとしてマウスのメソセリン抗体の作成

一方、C60の腹腔内投与による慢性的影響として腎臓への影響を示唆

$TiO_2$と C60の気管内投与による発がんプロモーション作用の示唆

**吸入試験法研究**

MWCNTのミスト暴露システムを開発

気管内投与時の分散性依存の発現様式差異を確認

リポソーム分散C60による気管内投与法を開発。

**暴露測定法／動態解析研究**

生体試料でのC60の定量的検出法との確立

静注後のC60の組織からの経時的消失検討

気管内投与後のMWCNTの肺及び肝臓での検出

***in vitro*試験法研究**

細胞培養系でのリポソーム等を用いた分散法の確立

→C60や$TiO_2$の遺伝毒性、細胞透過性、

神経系の細胞機能への影響、などへの適用

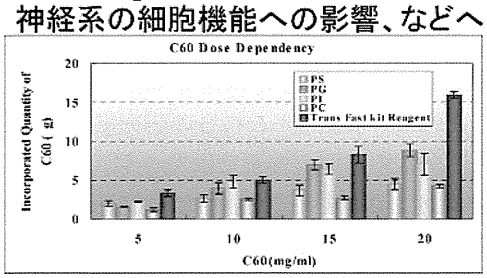


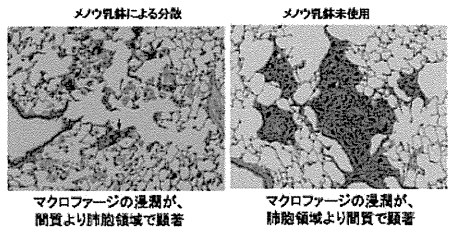


MWCNTの気管内投与後92日後の肺組織像

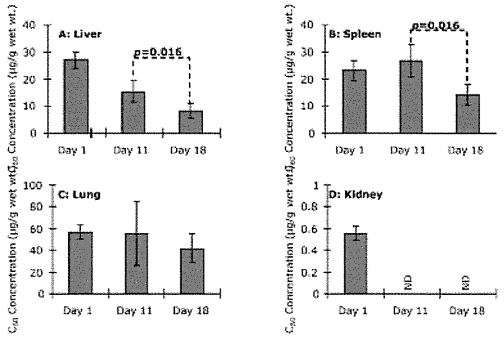


$C_{60}$のラットへの尾静脈投与(12.5 μg/kg)における体内分布
反復(4回)投与後の体内分布の経時変化

Fig. 2. The Overall Results of NIHS Projects for Nanomaterial Safety

長の長いタイプの多層型カーボンナノチューブ（MWCNT）が，中皮腫を誘発する可能性を持つことを確認した.[6] 上記の体内動態の重要性を考慮した概念からは，吸収性や体内分布について検証したのちに，慢性影響の可能性を検討することが論理的であるが，研究開始当時から，大量生産可能であった，酸化チタン（$TiO_2$）やフラーレン（C60），MWCNTについては，in vivoの慢性影響を先行して検討しておくべきであると判断した．特にその形状がアスベストに似ていたMWCNTについては，吸入曝露による有害影響が懸念されたが，MWCNTについての吸入曝露法が確立していない段階では，アスベストでも検証に使用されていた腹腔内投与による中皮腫誘発試験を行うこととした．

われわれの最初の実験は，アスベストで中皮腫の誘発時期が早くなることが知られているp53ヘテロノックアウトマウスへの腹腔内へ3 mg/ mouseという高用量を投与することによって確認されたものであり，動物種の特異性や投与量の多さについて異論も指摘された．しかしその後の研究で，野生型の動物種であるF344ラットに対しても，同じMWCNTが中皮腫の誘発作用を持つことが確認された[7]ほか，投与量を1000分の1にまで少なくした実験においても中皮腫の起きることが示されている（投稿中）．

酸化チタンについては，雌ラットへの吸入曝露により発がん性のあることが示されているが，ナノサイズ化による発がん性の検証のために，気管内投与による肺がんのプロモーション作用の検討を行った．その結果，酸化チタンは，肺腺腫や乳腺腫に対してプロモーション作用を示し，その作用は，マクロファージから放出される炎症性因子であるMIP1aを介したものであることが示唆された.[8] 現在C60やMWCNTを用いたプロモーション作用の検討が進行中である．

一方，曝露手法の開発においては，ミスト法や粉体法によるMWCNTの吸入曝露システムの開発研究を進めているが，より簡易な手法として気管内投与のための適切な分散法の検討を行った．その結果，分散法の違いが肺の有害性発現様式に違いを引き起こすことを確認した.[9]

体内動態解析のために，生体試料中のC60や$TiO_2$の分析手法の開発や改良を行い，経口投与や気管内投与による体内吸収性について検討を行っている．現在のところ投与部位である消化管や肺以外で有意な検出量を確認できておらず，感度の向上に向けた研究を進めている．しかし，体内への吸収を前提にした解析として，C60の静脈内投与による解析を行ったところ，肝臓や脾臓，肺などへの分布を確認したが，腎臓への分布は極めて低いことが示された（投稿中）．その他，遺伝毒性や標的臓器などの毒性をスクリーニングするためのin vitro試験における培地等への分散法も検討対象としており，リポソームを用いたC60の分散法を確立した．

### 4. 慢性影響研究の重要性

ナノマテリアルの生体影響に関する情報はここ数年の活発な研究状況を反映して多くなりつつあるが，慢性影響に関する報告は依然その数が少ない状況である．一般の化学物質の有害性評価の常套手段として，変異原性試験や短期試験から情報を収集していくことは，必要なステップであり，OECDにおけるナノマテリアル作業グループの活動におけるスポンサーシッププログラムにおいても，加盟各国からの毒性試験情報として，短期試験を中心に収集されてきている．われわれの研究グループにおいても，これらの枠組みに対して，短期的な試験情報を中心に提供し始めている段階である．しかしMWCNTに関しては，研究初期から，短期毒性より長期毒性の方が懸念の強いことが，物性等の情報から推測されたところでもあり，その推定に基づいて，腹腔内投与の研究を最初にスタートさせた．腹腔内投与は，リスク評価の観点からは，曝露経路（吸入曝露）に伴う定量的な評価に問題のあるところであるが，最近の注目すべき研究として，分散剤で分散させたMWCNT（最高80 mgまで）をマウスに吸引させた研究や，MWCNT: 30 mg/ $m^3$ をマウスに単回吸入曝露した研究において，曝露後7–8週間目にMWCNTが胸膜に到達していたことが報告されている.[10,11] これらの研究結果は高用量の曝露による短期間の結果ではあるが，呼吸器を経由した曝露においてもMWCNTは胸膜（中皮）まで到達することを示唆しており，われわれの腹腔内投与による結果と合わせると，リスク評価の上でも重要な知見であると考えられる．

これらの腹腔内投与による中皮腫誘発能は，繊維状粒子による催腫瘍性のみを検出する系であり，短

いタイプやその他様々な形状のMWCNTにおける慢性毒性は別途検証する必要性がある．実際，われわれの行った腹腔内投与試験では，小さいサイズのナノチューブ繊維を含んだ細胞が腹膜の病変部のみならず，肝類洞内，又は肝葉間や腸間膜リンパ節の中にも認められ，体内に再分布することが示唆された（Fig. 3）.[6] さらに，SWCNTをマウスへ咽頭吸引させた実験では，一過性の急性症状の後に，炎症性細胞浸潤を伴わない間質の繊維化が認められている.[12] また，ApoEノックアウトマウスを用いた実験では，タンパクカルボニル化活性の変化を伴うミトコンドリアDNA障害と，アテローム性動脈硬化症の進行を増強することが示された.[13] MWCNTに関しても，マウスにMWCNT（200-400 ng）を気管内滴下した実験では，一過性の肺の炎症反応に加え，投与量に依存した血小板の活性化と凝固作用の活性化の促進が示唆されている.[14] また，MWCNTやSWCNTの気管内投与や経鼻投与により，アレルギー反応の増強反応が報告されている.[15-17] これらの結果が，カーボンナノチューブが直接体内循環に侵入した結果であるか，免疫細胞との接触を介した反応であるかを区別することは難しいが，曝露局所に留まらない全身作用の可能性を示している．われわれの酸化チタンの気管内投与による発がんプロモーション作用が，炎症因子により介在されたことは，これらの知見と同様の作用様式を示すものととらえることもできる．

以上の知見は，短期の試験だけでは検証することは困難であり，ナノマテリアルの有害性を確認するためには，長期の体内動態予測や慢性影響に関する研究が，重要なステップであることを示している．Figure 4にスクリーニング試験や確定試験を開発するための手順についてまとめた．通常の化学物質については，その長い歴史の中で明らかとなった有害性に対して，それぞれの毒性発現様式に応じてスクリーニング試験が開発され，現在まで運用されてきている．特に変異原性試験は発がん性を予測する試験としての重要な役割を担っている．しかし，現時点ではナノマテリアルによる有害性影響が，これまでの研究経験の中で明らかとなった影響だけに留まるのかについては，まだ誰も判定できない状況である．これまでの一般化学物質に対応する有害性とスクリーニング試験を活用して進めていくと同時に，未知の影響を見極める最初のステップとして，少な

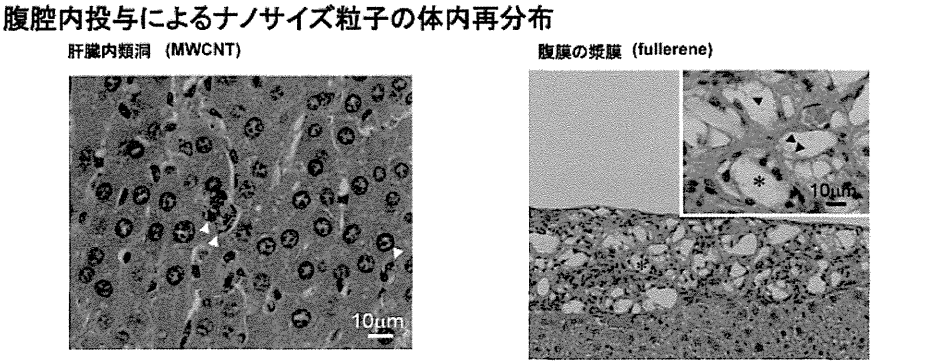


A. Takagi et al., J. Toxicol. Scie., **33**,105-116. (2008)

SWCNTやMWCNTによる全身性影響の示唆

- アテローム性動脈硬化症の進行の増強の可能性（ApoE$^{-/-}$マウス）
  Z. Li *et al.*, *Environmental health perspectives*. **115**, 377-382 (2007)
- 血小板の活性化と凝固作用の活性化（MWCNT気管内滴下）
  A. Nemmar *et al.*, *J. Thrombosis, Haemostasis* **5:** 1217-1226 (2007)
- アレルギー反応の増強（MWCNT・SWCNT、気管内・経鼻投与）
  E.J. Park *et al.*, *Toxicology*. **259**, 113-21 (2009)
  U.C. Nygaard *et al.*, *Toxicol Sci*. **109**, 113-23 (2009)
  K. Inoue *et al.*, *Toxicol Appl Pharmacol*. **237**, 306-16 (2009)

Fig. 3. The Suggestive Evidences for Systemic Toxicites by Nanomaterials

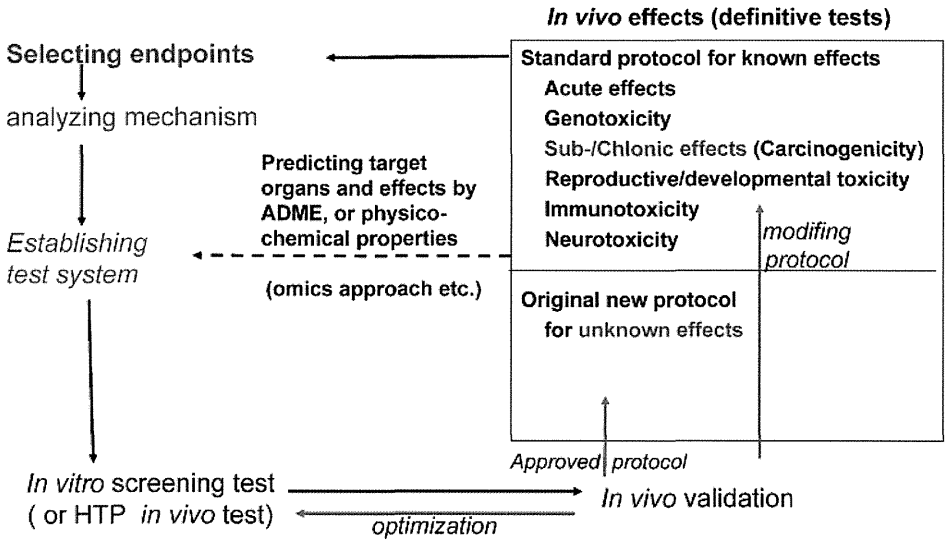


Fig. 4. The Schematic Development of Screening Tests and Definitive Tests

くとも代表的なナノマテリアルによる in vivo の慢性影響研究や，その影響を推定するためのナノマテリアルと生体成分との分子レベルでの相互作用や体内残留性様式の解析を進めていくべきであると考えられる．

**謝辞** 本稿で解説した研究成果の一部は，厚生労働科学研究費補助金（化学物質リスク研究事業）H17-化学-012，H18-化学--一般-007 及び H21-化学--一般-008 の助成によって行われたものです．

## REFERENCES

1) Scientific Committee on Emerging and Newly Identified Health Risks, SCENIHR: 〈http://ec.europa.eu/health/ph_risk/committees/04_scenihr/docs/scenihr_o_003b.pdf〉, European Commission Web, cited 14 November, 2010.
2) Scientific Committee on Emerging and Newly Identified Health Risks, SCENIHR: 〈http://ec.europa.eu/health/ph_risk/committees/04_scenihr/docs/scenihr_o_010.pdf〉, European Commission Web, cited 14 November, 2010.
3) Food Safety Authority of Ireland, FSA, ``The Relevance for Food Safety of Applications of Nanotechnology in Food and Feed Industries,'' Dublin, 2008.
4) UK Committees on Toxicity, Mutagenicity and Carcinogenicity of Chemicals in Food, Consumer Products and the Environment (COT, COM, COC): 〈http://cot.food.gov.uk/pdfs/cotstatements2005nanomats.pdf〉, COT Web, cited 14 November, 2010.
5) The Committee on Toxicity of Chemicals in Food, Consumer Products and the Environment: 〈http://www.food.gov.uk/multimedia/pdfs/cotstatementnanomats200701.pdf〉, cited 14 November, 2010.
6) Takagi A., Hirose A., Nishimura T., Fukumori N., Ogata A., Ohashi N., Kitajima S., Kanno J., J. Toxicol. Sci., 33, 105-116 (2008).
7) Sakamoto Y., Nakae D., Fukumori N., Tayama K., Maekawa A., Imai K., Hirose A., Nishimura T., Ohashi N., Ogata A., J. Toxicol. Sci., 34, 65-76 (2009).
8) Xu J., Futakuchi M., Iigo M., Fukamachi K., Alexander D. B., Shimizu H., Sakai Y., Tamano S., Furukawa F., Uchino T., Tokunaga H., Nishimura T., Hirose A., Kanno J., Tsuda H., Carcinogenesis, 31, 927-935 (2010).
9) Wako K., Kotani Y., Hirose A., Doi T., Hamada S., J. Toxicol. Sci., 35, 437-446 (2010).
10) Nurkiewicz T. R., Porter D. W., Hubbs A. F., Stone S., Chen B. T., Frazer D. G., Boegehold M. A., Castranova V., Toxicol. Sci., 110, 191-203 (2009).
11) Ryman-Rasmussen J. P., Cesta M. F., Brody

A. R., Shipley-Phillips J. K., Everitt J. I., Tewksbury E. W., Moss O.R., Wrong B. A., Dodd D. F., Andersen M. E., Bonner J. C., Nat. Nanotechnol., 4, 747-751 (2009).

12) Shvedova A. A., Kishin E. R., Mercer R., Murray A. R., Johnson V. J., Potapovich A. I., Tyurina Y. Y., Gorelik O., Arepalli S., Schwegler-Berry D., Hubbs A. F., Antonini J., Evans D. E., Ku B. K., Ramsey D., Maynard A., Kagan V. E., Castranova V., Baron P., Am. J. Physiol. Lung cell. mol. physiol., 289, L698-L708 (2005).

13) Li Z., Hulderman T., Salmen R., Chapman R., Leonars S. S., Young S. H., Shvedova A., Luster M. I., Simeonove P. P., Environ. Health Perspect., 115, 377-382 (2007).

14) Nemmar A., Hoet P. H., Vandervoort P., Dinsdale D., Nemery B., Hoylaerts M. F., J. Thromb. Haemost., 5, 1217-1226 (2007).

15) Park E. J., Cho W. S., Jeong J., Yi J., Choi K., Park K., Toxicology, 259, 113-121 (2009).

16) Nygaard U. C., Hansen J. S., Samuelsen M., Alberg T., Marioara C. D., Løvik M., Toxicol. Sci., 109, 113-123 (2009).

17) Inoue K., Koike E., Yanagisawa R., Hirano S., Nishikwa M., Takano H., Toxicol. Appl. Pharmacol., 237, 306-316 (2009).

J Occup Health 2011; 53: 51–63

Journal of Occupational Health

# Two- and 13-week Inhalation Toxicities of Indium-tin Oxide and Indium Oxide in Rats

Kasuke NAGANO[1], Kaoru GOTOH[1], Tatsuya KASAI[1], Shigetoshi AISO[1], Tomoshi NISHIZAWA[1], Makoto OHNISHI[1], Naoki IKAWA[1], Yoko EITAKI[2], Kenichi YAMADA[2], Heihachiro ARITO[1] and Shoji FUKUSHIMA[1]

[1]Japan Bioassay Research Center, Japan Industrial Safety and Health Association and [2]Occupational Health Research and Development Center, Japan Industrial Safety and Health Association, Japan

**Abstract: Two- and 13-week Inhalation Toxicities of Indium-tin Oxide and Indium Oxide in Rats: Kasuke NAGANO, *et al.* Japan Bioassay Research Center, Japan Industrial Safety and Health Association—Objectives:** Two- and 13-week inhalation toxicities of indium-tin oxide (ITO) and indium oxide (IO) were characterized for risk assessments of workers exposed to ITO. **Methods:** F344 rats of both sexes were exposed by inhalation to ITO or IO aerosol for 6 h/day, 5 day/wk for 2 wk at 0, 0.1, 1, 10 or 100 mg/m$^3$ or 13 wk at 0, 0.1or 1 mg/m$^3$. An aerosol generator and inhalation exposure system was constructed. **Results:** Blood and lung contents of indium were elevated in a dose-related manner in the ITO- and IO-exposed rats. ITO and IO particles were deposited in the lung, mediastinal lymph node and nasal-associated lymphoid tissue. Exposures to ITO and IO induced alveolar proteinosis, infiltrations of alveolar macrophages and inflammatory cells and alveolar epithelial hyperplasia in addition to increased lung weight. ITO affected the lung more severely than IO did. Fibrosis of alveolar wall developed and some of these lesions worsened at the end of the 26-week post-exposure period. **Conclusions:** Persistent pulmonary lesions including alveolar proteinosis and macrophage infiltration occurred after 2- and 13-week inhalation exposures of rats to ITO and IO. Fibrosis of alveolar wall developed later. These lesions occurred after ITO exposure at the same concentration as the current occupational exposure limit in the USA and at blood indium levels below the biological exposure index in Japan for indium.
(J Occup Health 2011; 53: 51–63)

Received Sep 17, 2010; Accepted Nov 15, 2010
Published online in J-STAGE Jan 11, 2011
Correspondence to: T. Nishizawa, Japan Bioassay Research Center, Japan Industrial Safety and Health Association, 2445 Hirasawa, Hadano, Kanagawa 257-0015, Japan
(e-mail: t-nishizawa@jisha.or.jp)

**Key words:** Indium-tin oxide, Indium oxide, Inhalation, Pulmonary toxicity, Rat

Indium-tin oxide (ITO), a sintered material containing 90% indium oxide (IO) and 10% tin oxide, has been extensively used in liquid-crystal displays and other display devices. The average annual growth of the use of indium in the form of ITO has increased by an average 18 percent per year[1]. The technology used to create ITO targets and ITO thin film applications gives rise to potential exposure to ITO particles, and poses a serious threat to the health of workers engaged in the manufacturing, processing and handling of ITO. Two fatal case studies have been reported. An operator of wet surface grinding in an ITO plant was diagnosed as interstitial pneumonia and died of bilateral pneumothorax[2], and a furnace operator in an ITO plant died of respiratory failure due to pulmonary alveolar proteinosis[3]. Recent epidemiological studies on the health of workers in ITO plants have demonstrated a potential cause of occupational lung disease as inhaled indium and an increased risk for interstitial lung damage by ITO inhalation[4–7]. Experimental toxicology studies have revealed that an administration of ITO causes persistent inflammation in the lung of rats[8], a strong cytotoxic response of macrophages in vitro by generation of reactive oxygen species (ROS)[8], and a pulmonary inflammatory response with diffuse bronchiolar and alveolar hyperplasia and interstitial fibrotic proliferation in hamsters[9,10]. An intratracheal administration of indium trichloride to rats was reported to initiate an inflammatory response with rapid development of fibrosis[11]. The National Toxicology Program's (NTP's) 14-week study[12] showed that inhalation exposure of rats to indium phosphide aerosol induces inflammation and alveolar proteinosis in the lung.

Inhalation is a principal route of exposure for workers in the facilities where ITO is manufactured, processed and

handled. In order to protect workers from inhalation exposure to indium and its compounds, an occupational exposure limit (OEL) of 0.1 mg/m$^3$ has been recommended as the Threshold Limit Value-Time Weighted Average (TLV-TWA) by the American Conference of Governmental Industrial Hygienists (ACGIH)[13], and as the Recommended Exposure Limit (REL) by the National Institute for Occupational Safety and Health (NIOSH)[14]. The Japan Society for Occupational Health (JSOH)[15] has recommended a serum indium level of 3 $\mu$g/l as a biological exposure index (BEI). It is of prime importance to provide basic animal toxicity data showing the dose-response relationships between concentrations of inhalation exposure of rats and mice to ITO and its major component, IO, target tissue doses of indium and resulting pulmonary toxic responses to these two aerosols.

In order to assess the health risks of workers exposed by inhalation to ITO and IO aerosols in the work environment, the present studies were intended to characterize subacute and subchronic inhalation toxicities of ITO and IO in rats and to provide dose-response relationships between aerosol concentrations of inhalation exposure to ITO and IO aerosols, lung and blood contents of indium and resulting pulmonary lesions. For this purpose, we constructed an aerosol generation and exposure system for providing inhalation exposure of unrestrained rats and mice to aerosols of ITO and IO at strictly controlled exposure concentrations ranging from 0.1 to 100 mg/m$^3$. And, we conducted inhalation exposures of male and female rats to dry aerosols of ITO and IO at these concentrations for 2 and 13 wk. A further purpose of the present studies was to predict an appropriate range of exposure concentrations of ITO aerosol for a 2-year rodent carcinogenicity study, based on the results.

## Materials and Methods

The present studies were conducted in accordance with the Organization for Economic Cooperation and Development's (OECD's) Good Laboratory Practice[16], and with reference to the OECD's Guidelines for Testing of Chemicals 412 "Repeated Dose Inhalation Toxicity, 28-day or 14-day Study"[17] and 413 "Subchronic Inhalation Toxicity, 90-day Study"[18]. The animals were cared for in accordance with the Guide for the Care and Use of Laboratory Animals[19] and the present studies were approved by the ethics committee of the Japan Bioassay Research Center.

### Test materials

Powders of ITO and IO were kindly supplied by JX Nippon Mining & Metals, Corp. (former Nippon Mining & Metals Co., Ltd.) (Tokyo, Japan). ITO powder was prepared by grinding the sintered ITO plate, and was colored with black. The mean diameter of the powder was 3.5 $\mu$m with a 90% cumulative diameter of 8.9 $\mu$m. The sintered ITO powder was composed of 90.06% IO and 9.74% $SnO_2$. Its purity was 99.8% with trace amounts of aluminium, chromium, copper, iron, nickel, lead, silica, zirconium and zinc as impurities. IO powder was colored with yellow, and had a mean diameter of 1.4 $\mu$m with a 90% cumulative diameter of 2.9 $\mu$m. The purity of the IO powder was 99.9% with trace amounts of tin, silica and lead as impurities.

### Animals

F344/DuCrlCrlj rats of both sexes were obtained at the age of 4 wk from Charles River Japan, Inc (Kanagawa, Japan). The animals were quarantined and acclimated for 2 wk before the start of experiment. The animals were housed individually in stainless-steel wire hanging cages (170 W × 294 D × 176 H mm), which were placed in a stainless steel inhalation exposure chamber of 1,060 liters in volume. The environment in the exposure chamber was maintained constant at a temperature of 20–24°C and a relative humidity of 30–70% with 12 air changes/h. The exposure chambers were installed in a barrier system animal room. Fluorescent lighting was controlled automatically to give a 12-hour light/dark cycle. All rats were given sterilized commercial pellet diet (CRF-1, Oriental Yeast Co., Ltd., Tokyo, Japan) and sterilized water ad libitum.

### Experimental design

In the 2-week study, groups of 5 rats of each sex were exposed to ITO or IO aerosol at a target concentration of 0.1, 1, 10 or 100 mg/m$^3$ as ITO or IO for 6 h/day, 5 day/wk for 2 wk. In the 13-week study, groups of 10 rats of each sex were exposed to ITO or IO aerosol at a target concentration of 0.1 or 1 mg/m$^3$ for 6 h/day, 5 day/wk for 13 wk. Groups of 5 or 10 rats of each sex were exposed to clean air for 2 or 13 wk under the same conditions, and served as respective controls. In order to evaluate recovery from the subchronic effects after cessation of the 13-week exposure to ITO, a post-exposure group of 10 rats of each sex was set up, which was exposed to ITO at 0.1 mg/m$^3$ for 13 wk and then to clean air for 26 wk. Ten rats of each sex serving as respective controls were handled in the same manner as the post-exposure group, but were exposed to clean air for 39 wk.

### Aerosol generation and exposure to ITO and IO

Two different systems for generation of ITO or IO aerosol and inhalation exposure were used in the present studies. A target aerosol concentration of 100 mg/m$^3$ was generated using a system illustrated in the upper part (A) of Fig. 1. It consisted of a dust feeder equipped with an ejector, an exposure chamber and a digital dust indicator (Type AP-632T, Sibata Scientific Technology, Ltd., Tokyo, Japan). Airflow containing the aerosol was generated by drawing the powder with compressed clean air at the first

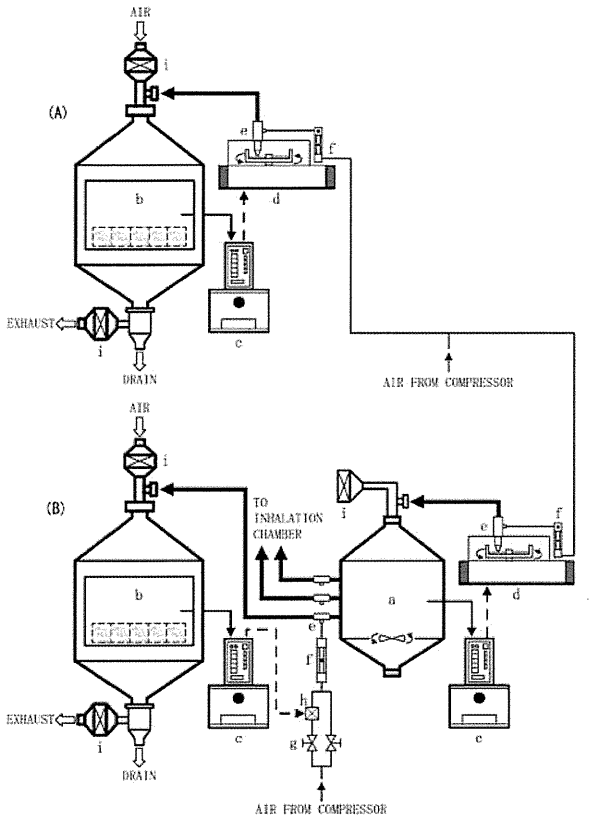


Fig. 1. A schematic diagram of the aerosol generation, regulation and inhalation exposure systems. (A) A system used for aerosol generation of a high aerosol concentration of 100 mg/m$^3$. (B) Another system used for generation of lower concentrations of 10, 1 and 0.1 mg/m$^3$. Thick, thin and dotted arrows indicate aerosol flow, sampling of chamber air for monitoring aerosol concentration and feedback control, respectively. Components of the systems: a) reservoir chamber, b) inhalation exposure chamber, c) digital dust indicator, d) dust feeder with an ejector, e) ejector, f) flowmeter, g) flow control valve, h) solenoid valve, i) HEPA filter.

ejector and introduced into the top of the exposure chamber where the filtered air had been kept flowing downward at 12 air changes/h. The mass-equivalent concentration of ITO or IO in the exposure chamber was monitored with the digital dust indicator. In order to keep the aerosol concentration constant in the exposure chamber during the 6-hour exposure period, a feedback control system between the digital dust indicator and the dust feeder was set up. When the chamber concentration went above an upper limit of a normal concentration range, the dust feeder stopped supplying the powder. Conversely, when the chamber concentration fell below the lower limit, the dust feeder started to supply the powder. Chamber concentrations of 10, 1 and 0.1 mg/m$^3$ were generated using another system illustrated in the lower part (B) of Fig. 1. It consisted of the first-stage system (a, c and d in Fig. 1B) for aerosol generation of a high concentration at 100 mg/m$^3$ and a further dilution system. Aerosol generation of the high concentration and its regulation were performed in the same manner described above, and airflow containing the aerosol was delivered to a reservoir chamber for stabilization of the aerosol concentration. The airflow containing the aerosol was delivered to the second ejector and then introduced into the top of the exposure chambers where the filtered air had been kept flowing downward at 12 air changes/h. The aerosol concentration in the exposure chamber was monitored with the second digital dust indicator and regulated at a target concentration of 10, 1 or 0.1 mg/m$^3$. The aerosol concentration was stabilized by setting up the second feedback system between the digital dust indicator and a solenoid valve which regulated the flow rate of compressed clean air entering the second ejectors. The exposure chambers were kept at a negative pressure (–100 Pa), in order to prevent leakage of ITO and IO aerosols into the outside air. Exhaust air from the exposure chamber was passed through a HEPA filter to remove ITO and IO particles before release into the atmosphere. The concentrations of indium in the exhaust air were below the detection limit of 0.0001 mg/m$^3$ after the treatment with the HEPA filter.

Chamber concentrations and size distribution of ITO and IO aerosols

In order to determine concentrations of ITO or IO aerosol in the exposure chamber, ITO or IO particles were collected on a filter (Teflon binder T60A20, Sibata Scientific Technology, Ltd, Tokyo, Japan) on Days 1 and 8 in the 2-week study and every week in the 13-week study. The particles on the filter were dissolved in a mixture solution of distilled water, hydrochloric acid and nitric acid (2:2:1 by volume ratio) at 160°C. The resulting solution was diluted with nitric acid, and then subjected to atomic absorption spectrometry analysis (Polarized Zeeman Atomic Absorption Spectrophotometer, Z-5010, Hitachi High-Technol. Co., Tokyo, Japan). Exposure chamber concentrations of ITO and IO aerosols were derived from the measured levels of elemental indium as shown in Table 1.

Measurement of the size distribution of ITO or IO aerosol in the exposure chamber was carried out once in the 2-week study and in the 4th and 8th wk in the 13-week study. ITO or IO aerosol was collected with an 8-stage Andersen sampler (Type AN200, Sibata Scientific Technology, Ltd). Using the mass of the particles on the filter (Teflon binder T60A20, Sibata Scientific Technology, Ltd) collected at each stage of the Andersen sampler, mass median aerodynamic diameter (MMAD) and geometric standard deviation (GSD) were determined.

Table 1. Mass concentrations and mass median aerodynamic diameters (MMADs) and geometric standard deviations (GSDs) of ITO and IO aerosols in the exposure chamber

| | ITO | | | | IO | | | |
|---|---|---|---|---|---|---|---|---|
| | Mass concentration ($mg/m^3$) | | Aerodynamic diameter | | Mass concentration ($mg/m^3$) | | Aerodynamic diameter | |
| Dose | (Mean ± SD) | | Median ($\mu m$) | GSD | (Mean ± SD) | | Median ($\mu m$) | GSD |
| 2-week study | | In a) | | | | In a) | | |
| 0.1 $mg/m^3$ | 0.09 ± 0.00 | 0.07 ± 0.00 | 2.5 | 1.8 | 0.10 ± 0.01 | 0.08 ± 0.01 | 1.9 | 1.7 |
| 1 $mg/m^3$ | 0.94 ± 0.02 | 0.70 ± 0.01 | 2.7 | 1.8 | 1.07 ± 0.06 | 0.89 ± 0.05 | 2.1 | 1.8 |
| 10 $mg/m^3$ | 9.33 ± 0.33 | 6.94 ± 0.25 | 3.0 | 1.8 | 10.76 ± 0.46 | 8.90 ± 0.38 | 2.1 | 1.8 |
| 100 $mg/m^3$ | 95.90 ± 2.99 | 71.35 ± 2.22 | 3.7 | 1.9 | 105.25 ± 7.01 | 87.04 ± 5.80 | 2.2 | 1.7 |
| 13-week study | | | | | | | | |
| 0.1 $mg/m^3$ | 0.10 ± 0.01 | 0.07 ± 0.01 | 2.4 | 1.8 | 0.10 ± 0.01 | 0.08 ± 0.01 | 2.1 | 1.7 |
| 1 $mg/m^3$ | 1.01 ± 0.08 | 0.75 ± 0.06 | 2.5 | 1.9 | 1.01 ± 0.09 | 0.84 ± 0.07 | 2.3 | 1.7 |

a): Mass concentration as indium.

### Determination of indium concentrations in the lung and blood

Lung indium was quantified in the 2-week study, and both the lung and whole-blood were analyzed for indium in the 13-week study. Cranial, caudal and accessory lobes of the right lung were used for the analysis. A sample of the lung or 1.0 ml of blood was added with ultra-pure nitric acid and digested with a microwave digestion apparatus (Microwave Digestion System, Model 7295, O·I·Analytical, CA, USA). The digested sample was added with ultra-pure water and injected into an inductively coupled plasma mass spectrometer (ICP-MS) (Type 7500i, Agilent Technologies, Ltd., CA, USA). Cesium was used as an internal standard for the indium measurement. The quantitative detection limit of indium was 0.006 $\mu g/g$ for lung tissue and 0.5 $\mu g/l$ for whole-blood. Lung indium was expressed as both a concentration of indium per gram of lung tissue and the content of indium in the whole-lung.

### Clinical observations and pathological examinations

The animals were observed daily for their clinical signs and mortality. Body weight and food consumption were measured weekly throughout the study periods. Animals surviving to the end of the 2- or 13-week exposure period and to the end of the 26-week post-exposure period received complete necropsy. Blood was collected for blood indium, hematology and blood biochemistry from the abdominal aorta under etherization. The organs and tissues designated in the OECD test guidelines[17, 18] were examined macroscopically and microscopically. The tissues were fixed in 10% neutral buffered formalin, and embedded in paraffin. Tissue sections of 5 $\mu m$ in thickness were prepared, and stained with hematoxylin and eosin (H & E). The sections of lung tissue were also stained with a periodic acid Schiff (PAS) reagent. Lesions of the lung and lymph nodes were evaluated for their severities, scoring on a scale of "slight" to "severe" with reference to the criteria of non-neoplastic lesions by Shackelford et al.[20].

### Statistical analysis

Body weight, organ weight, and hematological and blood biochemical parameters were analyzed by Dunnett's test as described previously[21]. Histopathological findings in the 13-week study were analyzed by chi-square test. A two-tailed test was used for all statistics. In all cases, a p value of 0.05 was used as the level of significance.

## Results

### Exposure chamber concentrations and size distributions of ITO and IO aerosol

Table 1 shows the mass concentrations derived from the measured levels of elemental indium (mean ± SD), MMADs and GSDs of ITO and IO aerosols in the exposure chamber. The exposure concentrations of ITO and IO aerosols were found to be regulated precisely within less than 10% in the variation coefficient and accurately within less than 10% deviation from the target concentrations. MMADs of the ITO aerosol tended to slightly increase with an increase in the chamber concentrations, while the GSDs were constant at all exposure concentrations. On the other hand, MMADs and GSDs of IO aerosol were constant over a wide range of exposure concentrations, and MMADs of IO aerosol were slightly smaller than those of ITO aerosol.

### Indium concentrations in the lung and blood

Table 2 shows lung and blood contents of indium in the male and female rats exposed to ITO and IO for 2 and 13 wk. Lung contents of indium expressed as $\mu g/g$ lung tissue and $\mu g$/whole-lung were increased with an increase in the concentration of exposure to ITO or IO, but the exposure concentration-related increase was smaller in the unit of $\mu g/g$ lung tissue than in that of $\mu g$/whole-lung, because the lung weights of the exposed rats were significantly heavier, up to 2-fold heavier than those of the control groups, depending on the exposure concentration (Fig. 2). In the 2-week study, the whole-lung contents of indium in the

Table 2. Lung and blood contents of indium in the male and female rats exposed to ITO or IO at 4 different concentrations for 2 wk, in those exposed to ITO or IO at 0.1 or 1 mg/m³ for 13 wk, and in those exposed to ITO at 0.1 mg/m³ for 13 wk followed by exposure to clean air for 26 wk

| | 2-week study | | | | 13-week study | | |
|---|---|---|---|---|---|---|---|
| Group name (mg/m³) | 0.1 | 1 | 10 | 100 | 0.1 | 0.1 (P) | 1 |
| No. of animals examined | 5 | 5 | 5 | 5 | 10 | 10 | 10 |
| <ITO> | | | | | | | |
| Male | | | | | | | |
| Lung (μg/g as In) | 3.3 ± 0.3 | 32.4 ± 2.7 | 127.6 ± 17.7 | 470.3 ± 58.1 | 24.0 ± 2.7 | 8.8 ± 1.1 | 74.4 ± 10.5 |
| Lung (μg/whole-lung as In) | 2.4 ± 0.1 | 31.1 ± 1.8 | 165.1 ± 9.8 | 688.3 ± 43.1 | 38.7 ± 4.6 | 15.0 ± 2.0 | 173.9 ± 28.6 |
| Blood (μg/l as In) | – | – | – | – | 0.77 ± 0.09 | 1.04 ± 0.10 | 3.39 ± 0.33 |
| Female | | | | | | | |
| Lung (μg/g as In) | 2.9 ± 0.4 | 34.8 ± 8.8 | 148.0 ± 41.2 | 533.9 ± 69.1 | 22.9 ± 2.2 | 8.6 ± 1.0 | 79.9 ± 7.1 |
| Lung (μg/whole-lung as In) | 1.8 ± 0.2 | 28.1 ± 7.2 | 157.4 ± 41.9 | 658.7 ± 70.9 | 26.3 ± 2.7 | 10.3 ± 1.1 | 134.6 ± 8.0 |
| Blood (μg/l as In) | – | – | – | – | 1.13 ± 0.32 | 1.46 ± 0.26 | 4.06 ± 0.56 |
| <IO> | | | | | | | |
| Male | | | | | | | |
| Lung (μg/g as In) | 5.3 ± 0.5 | 61.3 ± 11.1 | 261.7 ± 7.2 | 1124.7 ± 49.3 | 18.0 ± 2.3 | – | 144.2 ± 15.7 |
| Lung (μg/whole-lung as In) | 3.7 ± 0.3 | 45.1 ± 5.7 | 324.5 ± 20.0 | 1689.2 ± 64.2 | 17.2 ± 2.8 | – | 235.5 ± 34.0 |
| Blood (μg/l as In) | – | – | – | – | ND | – | 0.76 ± 0.08 |
| Female | | | | | | | |
| Lung (μg/g as In) | 5.0 ± 0.3 | 52.8 ± 3.2 | 267.0 ± 25.5 | 1190.8 ± 51.0 | 13.4 ± 1.5 | – | 130.6 ± 15.7 |
| Lung (μg/whole-lung as In) | 3.1 ± 0.2 | 33.8 ± 3.2 | 263.8 ± 26.7 | 1464.1 ± 88.2 | 9.8 ± 1.0 | – | 157.3 ± 17.4 |
| Blood (μg/l as In) | – | – | – | – | ND | – | 0.96 ± 0.26 |

(P): Data at the end of the 26-week post-exposure period. Values indicate mean ± SD. ND: Contents were below the quantitative detection limit (0.5 μg/l). –: Not examined.

ITO- and IO-exposed groups of both sexes were not increased in a manner proportional to the exposure concentration. The whole-lung contents of indium were lower in the ITO-exposed groups than in the IO-exposed groups of both sexes at all exposure concentrations. In the 13-week study, the exposure concentration-related increase in the whole-lung content of indium was also disproportionately lowered to greater extent in the ITO-exposed rats than in the IO-exposed rats. Unlike the result from the 2-week study, the whole-lung contents of indium in the 0.1 mg/m³ ITO-exposed rats of both sexes were higher than those of the 0.1 mg/m³ IO-exposed rats of both sexes. The whole-lung contents of indium in the ITO-exposed rats of both sexes measured at the end of the 26-week post-exposure period were lowered to 40% as compared with those measured at the end of the 13-week exposure.

Table 2 also shows the blood contents of indium in the male and female rats at the end of 13-week exposures to ITO and IO at 0.1 and 1 mg/m³ as well as those exposed to ITO at 0.1 mg/m³ for 13 wk and then to clean air for 26 wk. The blood contents of indium in the 0.1 mg/m³ IO-exposed rats of both sexes were below the quantitative detection limit of 0.5 μg/l. The blood contents of indium in the 1 mg/m³ ITO-exposed groups of both sexes were 4-fold higher than those in 1 mg/m³ IO-exposed group of both sexes. The blood contents of indium in the 0.1 mg/m³ ITO-exposed rats of both sexes measured at the end of the 26-week post-exposure period were 1.3-fold higher than those measured at the end of the 13-week exposure period.

Mortality and clinical signs in the 2- and 13-week studies

Neither death nor abnormal clinical sign, such as irregular sounds of respiration, was observed in any group exposed to ITO or IO for 2 or 13 wk. There was no growth retardation in any group exposed to ITO or IO for 2 or 13 wk as compared with the growth rate in the respective control.

Hematological and blood biochemical changes in the 2- and 13-week studies

In the 2-week study, white blood cell counts in the 100

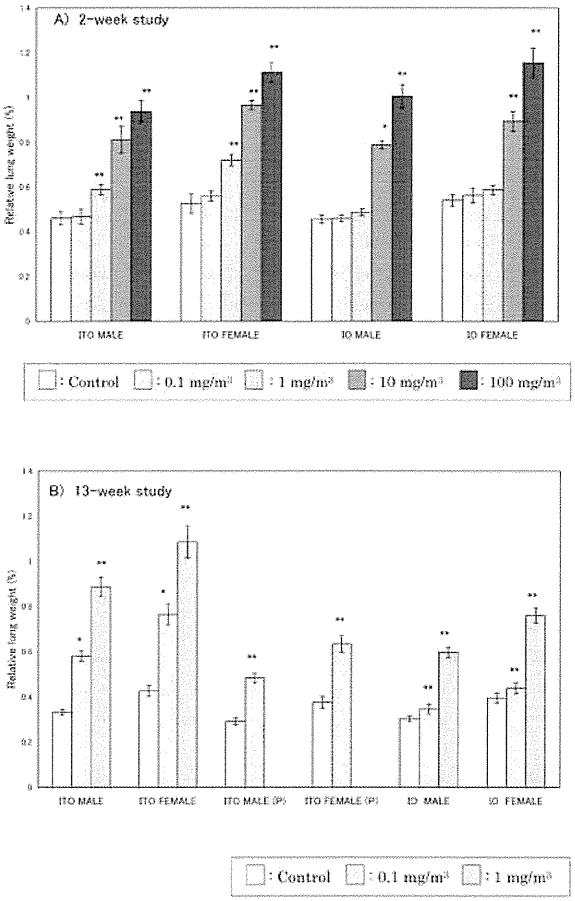


Fig. 2. Relative lung weights: A) in the rats of both sexes exposed to ITO or IO aerosol at 0, 0.1, 1, 10 or 100 mg/m$^3$ for 2 wk, B) in the rats of both sexes exposed to ITO or IO aerosol at 0, 0.1 or 1 mg/m$^3$ for 13 wk. (P) represents the rats of both sexes exposed to ITO aerosol at 0 or 0.1 mg/m$^3$ for 13 wk and subsequently to clean air for 26 wk.

mg/m$^3$ ITO-exposed male rats and red blood cell counts, hemoglobin and hematocrit values in the 100 mg/m$^3$ IO-exposed male rats were significantly increased compared with the respective control groups. In the 13-week study, potassium was significantly decreased in both 0.1 and 1 mg/m$^3$ ITO- and IO-exposed rats. In addition, significant decreases in sodium and chlorine in the 0.1 and 1 mg/m$^3$ IO-exposed male rats and significantly decreased triglyceride in the 0.1 and 1 mg/m$^3$ IO-exposed female rats were also observed (data not shown).

*Pathological findings in the 2-week study*

Relative lung weights were significantly increased in the male and female rats exposed to ITO at 1 mg/m$^3$ and above compared with the respective control groups, whereas significantly increased lung weights were noted in the rats of both sexes exposed to IO only at 10 and 100 mg/m$^3$ compared with the respective control groups (Fig. 2-A). Increases in absolute lung weights were indicated as well (data not shown).

Microscopic examination revealed that ITO and IO particles were deposited in the lungs of all the exposed rats except those exposed to the 0.1 mg/m$^3$ (Table 3). The particles were pale brown and transparent, looked like amber, and were located primarily within the alveolar macrophages (Fig. 3-1) and partly as a free form in the alveolar space. Both ITO and IO particles were deposited separately as single particles. ITO and IO particles were also observed to lesser extent in the bronchus-associated lymphoid tissue (BALT) of the lung, in the mediastinal lymph nodes (MLN) and in the nasal-associated lymphoid tissue (NALT) of the nasopharyngeal duct. The particles were located within macrophages, and notably, degenerative alveolar macrophages engulfing the particles were often observed (Fig. 3-1). The most remarkable lesion found in the present 2-week study was alveolar proteinosis characterized by filling of the alveolar space with a granular, pale eosinophilic material in the ITO- and IO-exposed rats. The diagnosis of alveolar proteinosis was based on the positive staining of eosinophilic material in the alveolar space with a PAS reagent. Alveolar proteinosis was observed in the 1, 10 and 100 mg/m$^3$ ITO-exposed rats and in the 10 and 100 mg/m$^3$ IO-exposed rats, and its severity score was increased dose-dependently in both the ITO- and IO-exposed groups. Incidences of alveolar macrophage infiltration in the ITO and IO-exposed rats were increased at the same exposure concentrations as the occurrence of alveolar proteinosis. Infiltration of inflammatory cells which were primarily composed of neutrophils and lymphocytes was observed in the alveolar space and wall of almost all the 10 and 100 mg/m$^3$ ITO- and IO-exposed rats of both sexes. Hyperplasia of alveolar epithelium occurred in some 10 and 100 mg/m$^3$ ITO- and IO-exposed rats, and was characterized by increased numbers of cuboidal cells, which were assumed to be type II pneumocytes, and by their location in the focal lung areas accompanied by infiltrations of alveolar macrophages and inflammatory cells. Those alveolar macrophages had foamy cytoplasm.

*Pathological findings in the 13-week study*

Relative lung weights were significantly increased in all the rats of both sexes exposed to ITO and IO at 0.1 and 1 mg/m$^3$ compared with the respective control groups (Fig. 2-B). The increase in the relative lung weight was more marked in the ITO-exposed rats of both sexes than in the IO-exposed rats. Increases in absolute lung weights were observed as well (data not shown).

Microscopic examination revealed that ITO and IO particles were deposited in the lungs of all the exposed